

Developing Trajectory Planning with Behavioral Cloning and Proximal Policy Optimization for Path-Tracking and Static Obstacle Nudging

Mingyan Zhou¹, Biao Wang¹, Xiatao Sun²

Abstract—End-to-end approaches with Reinforcement Learning (RL) and Imitation Learning (IL) have gained increasing popularity in autonomous driving. However, they do not involve explicit reasoning like classic robotics workflow, nor planning with horizons, leading strategies implicit and myopic. In this paper, we introduce our trajectory planning method that uses Behavioral Cloning (BC) for path-tracking and Proximal Policy Optimization (PPO) bootstrapped by BC for static obstacle nudging. It outputs lateral offset values to adjust the given reference trajectory, and performs modified path for different controllers. Our experimental results show that the algorithm can do path-tracking that mimics the expert performance, and avoiding collision to fixed obstacles by trial and errors. This method makes a good attempt at planning with learning-based methods in trajectory planning problems of autonomous driving.

I. INTRODUCTION

A. Background

Reinforcement Learning (RL) is a machine learning paradigm where an agent learns optimal behaviors through interactions with its environment, typically framed as a Markov Decision Process (MDP). Among RL algorithms, Policy Gradient methods are notable for their effectiveness in model-free scenarios. Vanilla Policy Gradient (VPG) [1] serves as a foundational approach, parameterizing and updating the policy in the direction of the expected rewards gradient. Trust Region Policy Optimization (TRPO) [2] enhances stability by constraining policy updates with KL-divergence, while Proximal Policy Optimization (PPO) [3] simplifies optimization while maintaining stability, leading which to become one of the most popular RL algorithms.

Imitation Learning (IL) involves training an agent to replicate behaviors from expert demonstrations [4] instead. Behavioral Cloning (BC), the foundational IL method was first introduced by [5] using Supervised Learning. BC is simple and efficient, especially for learning reactive behaviors and when the expert covers all state spaces, minimizing the impact of one-step deviations. However, it struggles with sequential prediction problems, leading to compounding errors in long-term tasks. Covariate shift results in distribution mismatch, undermining the performance of BC. To address these issues, methods like Data Aggregation (Dagger) [6], Human-Gated Dagger (HG-Dagger) [7], and Expert Intervention Learning (EIL) [8] have been invented.

¹ Mingyan Zhou is with the Department of Electrical and Systems Engineering, Biao Wang is with the Department of Mechanical Engineering and Applied Mechanics, University of Pennsylvania, Philadelphia, PA 19104, USA (e-mail: {derekzmy, wangbiao}@alumni.upenn.edu).

² Xiatao Sun is with the Department of Computer Science, Yale University, New Haven, CT 06510, USA (e-mail: xiatao.sun@yale.edu).

Beyond theoretical developments, numerous applications have demonstrated the potency of RL and IL, particularly in the field of robotics, including quadrotors [9], autonomous vehicles [10], robotic arms [11] etc. Among different robotics platforms, many have been developed for educational and research purposes for autonomous driving with RL and IL methods. AutoRally [12] developed Deep IL for off-road driving, [13] built up a 1/20 th scale vehicle with an onboard Jetson Nano for validating RL-based algorithms. Among these various autonomous driving platforms, FITENTH [14] stands out as one of the most promising. It features reliable hardware for cost-efficient validation, a reproducible simulation environment for rapid implementation, and a wealth of open-source materials accumulated from extensive developer contributions. Significant research have been achieved using FITENTH platform, including high-speed control [15], generalized RL [16], safe overtaking [17] etc.

B. Motivation

Classic autonomous driving software pipelines are modularly developed, comprising distinct components such as perception, planning, control, and so on [18]. For instance, the AV4EV go-kart [19] is designed for 1/3th scaled autonomous racing and offers a comprehensive robotics workflow. Besides robotics pipeline, end-to-end methods are gaining popularity in autonomous driving research due to the simplified and efficient design, as well as the potential for continuous improvement. End-to-end methods involve replacing either partial or all software modules with data-driven approaches, including various types of RL and IL methods.

For end-to-end approaches developed on the FITENTH, [20] demonstrates a successful implementation of PPO, using downsampled lidar data as input and producing steering and speed commands as output. Similarly, [21] showcases the feasibility and the benchmark comparison of DPL methods. However, there are two points that can be addressed. First, the explainability is limited. Deep learning methods often operate as black boxes, making it challenging to interpret and understand specific decision-making processes. This reduced transparency complicates reasoning and further validation. Second, without accounting for the horizon for planning, these approaches exhibit myopic behavior, causing the vehicle to respond reactively as noted in [22], which may fall into edge cases or become overly reliant on inputs. This issue is especially noticeable on straight-line tracks and in real-world scenarios, despite efforts such as fine-tuning penalties in reward functions and additional training and labeling.

To address opaque decision-making, partial end-to-end

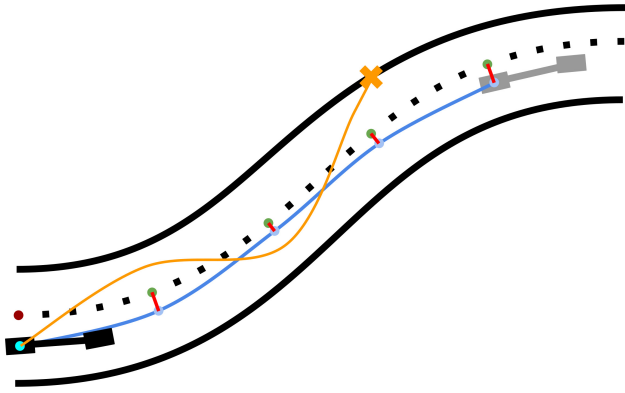


Fig. 1: Path-tracking through trajectory-planning-based BC. Given demonstration (blue trace) from the expert (single-track model in grey), instead of deviation or collision (yellow marks), the vehicle (single-track model in black) learns to mimic the expert by adjusting lateral offsets (red line segments) on the selected trajectory (green dots) obtained by current state (cyan dot), reference waypoints (black dots), and closest waypoint (crimson dot).

methods replace specific modules within the autonomous driving software pipeline, narrowing down the learning-based approach to particular tasks, such as methods introduced in [23] and [24] for path-planning problems. Hence, decoupling rule-based methods among robotics workflow while concentrating on specific modules like planning or on specific tasks like obstacle avoidance can be a promising area for exploration. On the other hand, to enhance trajectory planning with RL and IL in order to move beyond reactive performance, one of the encouraging methods is shifting outputs from steering and speed commands to sequences of data such as lateral offsets or a series of actions. This enables a prediction for motion planning in a longer term. Additionally, prior research in [21] have demonstrated the strong bootstrapping capabilities of IL methods for achieving fast convergence and improved performance, especially for bootstrapping PPO. Thus, integrating bootstrapping is also beneficial.

C. Contributions

This work makes three main contributions:

- 1) We propose a novel approach that improve planning to "planning with learning" as an integrated component of the robotics workflow for autonomous driving;
- 2) We adopt Behavioral Cloning (BC) algorithm on trajectory planning for path-tracking tasks, and the deployment is compatible with different path-tracking controllers (Fig. 1);
- 3) We utilize the Proximal Policy Optimization (PPO) algorithm bootstrapped by BC to modify reference waypoints with lateral offsets to achieve static obstacle nudging (Fig. 2).

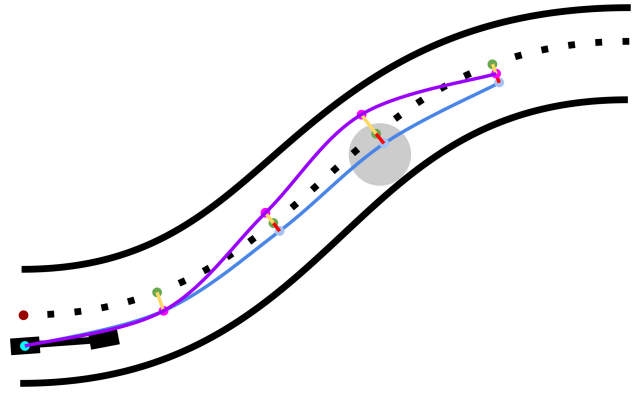


Fig. 2: Static obstacle nudging through trajectory planning-based PPO. After bootstrapping by BC as illustrated in Fig. 1, the vehicle performs planning similar to the expert's (blue trace). To avoid obstacles (grey circle) that may block the trajectory, the vehicle adopts PPO to adjust the policy that outputs offsets to get a new trajectory (purple trace), which reflects as adding new deviations (yellow line segments) to get new waypoints (pink dots).

II. METHODOLOGY

Based on classic robotics workflow, we build up the process for path-tracking and static obstacle nudging respectively as depicted in Fig. 3 and Fig. 4. The localization module provides current state of the vehicle for other modules, and the perception part outputs lidar scans for sensing the environment. Raceline, or reference waypoints, is generated beforehand as the offline planning data for purpose of truncating reference trajectory. BC and PPO part, working as a "planning with learning" module, receive three types of data and outputs offsets to get the modified trajectory. Finally, the controller uses the modified trajectory to maneuver the vehicle with calculated steering and speed commands.

A. Kinematic Bicycle Model

Following the standard formalism of vehicle modeling, we simplify the Ackermann-steered vehicle as a single-track kinematic model [25], where we have the center of the rear axle as vehicle position in 2D coordinates (x, y) , steering angle δ , heading angle or orientation θ , and wheelbase distance L_{wb} . Suppose no side slip, we denote the car's longitudinal velocity as v . Therefore, we define the vehicle state \mathbf{s} and desired action \mathbf{a} as follows:

$$\mathbf{s} = [x, y, v, \theta], \quad \mathbf{a} = [\delta_{des}, v_{des}].$$

B. Lidar Scan

We define lidar scan data as $\mathbf{S}_p \in \mathbb{R}^k$, where k denotes the number of lidar beams projected in the polar coordinates. To express the data more explicitly, we transform \mathbf{S}_p into Cartesian frame of the vehicle:

$$\mathbf{S} = T_p^c \mathbf{S}_p. \quad (1)$$

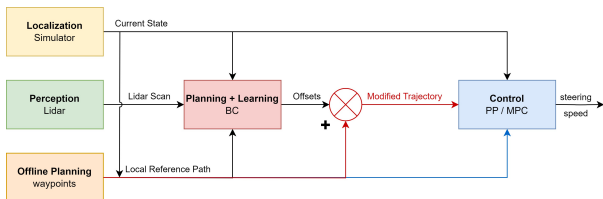


Fig. 3: Structure of path-tracking with trajectory-planning-based BC. Controller directly takes the trajectory from waypoints as reference (blue lines) to train the policy. During Validation process, offsets are added up the to get the modified trajectory for controller (red lines).

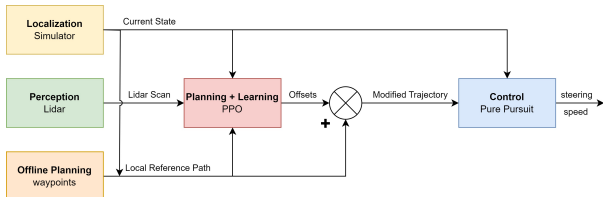


Fig. 4: Structure of static obstacle nudging with trajectory-planning-based PPO. Bootstrapped policy by BC is trained and tested using PPO to output lateral offsets for modifying trajectories, thereby avoiding obstacles.

\mathbf{S} is the lidar data in local Cartesian frame, and T_p^c indicates the frame transformation.

C. Waypoints

We define waypoint data as $\mathbf{w} \in (\mathbb{R}^5)^n$, where

$$w_i = [x_i, y_i, v_i, \theta_i, \gamma_i], \quad i = 1, \dots, n$$

denotes the coordinates, the reference longitudinal speed, the heading angle, and the curvature of the i th waypoint in n waypoints. Following waypoints as a reference path, the vehicle proceeds tracking.

In order to generate a global raceline for better reference, we apply an algorithm proposed in [26] as

$$\min_{[\alpha_1 \dots \alpha_n]} \sum_{i=1}^n \gamma_i^2(t) \quad (2)$$

$$\text{s.t. } \alpha_i \in [\alpha_{i,\min}, \alpha_{i,\max}]. \quad (3)$$

Through optimization parameter α_i that indicates the relative lateral position of track boundaries, it minimizes the squared sum of every curvature γ_i at time t of spline between every adjacent waypoints. Hence, we can get the optimal raceline as waypoints for references.

D. Trajectory Planning

Suppose H is the planning horizon and Δt is the step time. Based on vehicle position (x, y) , we extract the waypoint coordinates the car will go in $H \cdot \Delta t$ time with H steps as $(x, y)_i, \dots, (x, y)_j$. We interpolate these waypoints and evenly sample H points including endpoints, and note as horizon trajectory \mathbf{t}_h . Through homogeneous transformation T_w^c , we get local horizon trajectory. After adding offsets \mathbf{o} generated

by learning methods, we transform the trajectory with offset back to the world frame through T_w^c to get the modified trajectory \mathbf{t}_m in world frame:

$$\mathbf{t}_m = T_c^w (T_w^c \mathbf{t}_h + \mathbf{o}). \quad (4)$$

With \mathbf{t}_m , the path-tracking controllers can take the modified trajectory as new reference path to perform the obstacle nudging.

E. BC for Path-Tracking

BC can be formulated through Supervised Learning as eq.(5a), where the difference between the learned policy π and expert demonstrations generated by the expert policy π^* are minimized through loss function \mathcal{L} with respect to some metric, and $\hat{\pi}^*$ is the approximated policy.

$$\hat{\pi}^* = \operatorname{argmin}_{\pi} \sum \mathcal{L}(\pi(\mathbf{s}), \pi^*(\mathbf{s})) \quad (5a)$$

$$= \operatorname{argmin}_{\pi} \sum_{j=1}^t \sum_{i=1}^H |o_i| \quad (5b)$$

Here, agent policy is $\pi(\mathbf{s}) = \mathbf{o}$, denotes the lateral offsets corresponding to $T_w^c \mathbf{t}_h$. Consider system dynamics and other factors, reference waypoints cannot be tracked perfectly even for the expert. However, the deviation is miscellaneous that can be ignored to simplify the calculation. L1 norm can be used as the metric to express the deviations, and the norm value in every time step can be added up as the loss function, shown as eq.(5b).

By solving this optimization problem, the policy output is trained from penalizing random sampling and large deviations to converging to the expert performance with waypoint trajectory. This can be used for bootstrapping RL methods with rapid convergence and enhanced performance.

F. PPO for Static Obstacle Nudging

To achieve static obstacle nudging using waypoint data, lidar scans, and the current state with a bootstrapped model, we have to move away from BC and other IL methods. This is because even expert demonstrations fall short for these tasks. Instead, we use PPO to train the policy through balancing exploration and exploitation. By focusing on policy performance without direct access to the environment, we chose policy optimization methods, specifically PPO, due to its proven performance and mature development.

In general, PPO optimizes the policy through

$$\alpha_{k+1} = \operatorname{argmax}_{\alpha} E [\min(\frac{\pi_{\alpha}}{\pi_{\alpha_k}} A, g)], \quad (6)$$

where α_k denotes the policy parameters during iteration k , A is the advantage for the current policy π_{α_k} , and g is the clipping function. We refer to the implementation of CleanRL [27] with further details.

Optimizing the policy through PPO, instead of generating steering and speed commands like [21], the policy outputs \mathbf{o} , which deviate \mathbf{t}_h to be the modified trajectory \mathbf{t}_m . \mathbf{t}_m are then executed by Pure-Pursuit, a path-tracking method, thus achieving fixed obstacle nudging.

G. Path-tracking Controllers

Pure-Pursuit To pursue the goal, a lookahead point is determined from a fixed lookahead distance L towards the desired path. Based on the kinematic bicycle model, we utilize the geometric relationship between δ and the turning radius r , and subsequently derive the arc curvature γ :

$$\gamma = \frac{1}{r} = \frac{\tan\delta}{L_{wb}} = \frac{2|e|}{L^2}, \quad (7)$$

where $|e|$ is the cross-track error from the vehicle to the lookahead point, which coordinates are provided by the reference trajectory. Therefore, we can solve for δ , and achieve tracking the waypoints.

Model Predictive Control By building up a optimization problem with physical constraints and state dynamics, MPC can solve for a sequence of action. We define the state z and input u based on the single-track kinematic model as

$$z = [x \quad y \quad v \quad \theta]^T, \quad u = [a \quad \delta]^T,$$

where a is the desired vehicle acceleration. By discretization and linearization, we derive the system dynamics, and we formulate the objective along constraints as

$$\begin{aligned} \min \quad & \sum_{t=0}^{H-1} (z_t - z_t^r)^T Q_t (z_t - z_t^r) \\ & + (z_H - z_H^r)^T Q_H (z_H - z_H^r) \\ & + \sum_{t=0}^{H-1} (u_t - u_t^r)^T R_t (u_t - u_t^r) + \sum_{t=0}^H u_t^T R_d u_t \quad (8) \\ \text{s.t.} \quad & z_{t+1} = Ax_t + Bu_t + C \quad (9a) \\ & z_0 = z_{cur}, \quad z_{min} \leq z_t \leq z_{max} \quad (9b, 9c) \\ & u_{min} \leq u_t \leq u_{max}, \quad u'_{min} \leq u'_t \leq u'_{max}. \quad (9d, 9e) \end{aligned}$$

In (8), Q_t , Q_H stand for step and final penalty matrix of z , R_t , R_d are step and differential penalty matrix of u . (9a) indicates the system dynamics with system matrices A , B , C [28]. (9b) requires the initial condition is the current state z_{cur} , (9c, 9d) limit z_t , u_t respectively, and (9e) constrains the difference of u_t . The vehicle executes solved u_t , which is a and δ for tracking.

III. EXPERIMENTS

In this section, we present a detailed implementation and verification through experiments in simulation scenarios. We demonstrate that the trajectory-planning-based BC and PPO bootstrapped by BC achieve great performance in path-tracking and static obstacle nudging respectively. The implementation of code, video links, instructions, and additional resources are available at <https://github.com/derekhambaliq/Planning-with-Learning>.

A. Experimental Setup

We conduct development and verification on `fltenth_gym`, a simulation environment of `F1TENTH` based on `Gym`. `fltenth_gym` offers a robust closed-loop simulation framework facilitating rapid implementation. To incorporate

learning-based methods, we integrate the single-file PPO implementation from `CleanRL` [27] into `fltenth_gym`, enabling the use of PPO.

The experimental setup is deployed following different aspects. Hokuyo lidar scan data is downsampled from 1080 to 108 beams as in [21] to reduce the input dimension of the model. The trajectory prediction time is set to 1 s and 2 s for path-tracking and static obstacle nudging respectively. The planning horizon is $H = 10$ for evaluating the planning process. The vehicle's initial pose is randomized along reference waypoints, maintaining the same orientation and avoiding collisions. For Pure Pursuit, the vehicle is configured with a fixed lookahead distance of $L = 0.8$ m and a constant speed of 2 m/s to ensure stable performance. In line with Pure Pursuit, the speed of MPC is capped with a maximum of 2 m/s. Additionally, the control frequency is set to 10 Hz.

The agent model is actor-critic, compatible with PPO design. The critic network learns the value function, which estimates the expected reward of being in a particular state; the actor network outputs the mean of the action distribution. Two networks embrace same network structure, which is a 4×256 Multi-layer Perceptron. The learning rate is 3×10^{-4} , the general advantage estimation is 0.95, and the discount factor is 0.99. Maximum Gradient Norm is set to 0.5 to prevent gradient explosions. To design the reward function, we calculate the reward r based on the following values: the vehicle's longevity accumulated through the number of step time (0.01 s) n without crashing or finishing the laps, the 2-norm penalty of offsets \mathbf{o} , and the collision penalty $C = 1000$. The reward function shows as follows:

$$r = 100 \cdot n - \|\mathbf{o}\|_2 - C, \quad (10)$$

B. Path-Tracking with BC

We train agents using demonstration data that use controllers of Pure Pursuit and MPC separately. To compare the performance of two experiments, we set the prediction time to 1s, consistent with the MPC system dynamics setup. The total number of training time steps for BC is set to 1 million and 2 millions for comparisons.

For the training result, the episodic returns, shown in Fig. 6, illustrate the rapid convergence and learning efficiency of BC. With additional training, the models have higher return values than the models trained with 1 million. Besides, 2 million models reach to nearly the same return value, indicating the "planning with learning" method is compatible with different path-tracking controllers. Fig. 5 illustrates the modified trajectories are close to reference waypoints, showing the great performance of path-tracking through BC. With extended training, the trajectories predicted by agents become smoother with less deviation, which is also evident depicted in Fig. 6.

C. Static Obstacle Nudging with PPO

Static obstacle nudging is achieved by adjusting selected reference waypoints through lateral offsets \mathbf{o} . To illustrate trajectory deviations from the horizon trajectory, we bootstrap a model using BC with Pure Pursuit demonstrations.

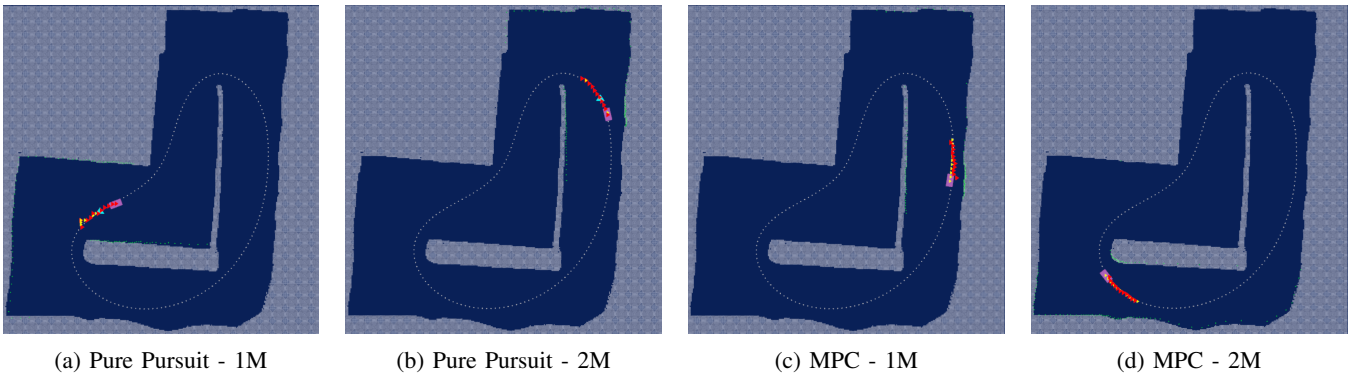


Fig. 5: BC performance for path-tracking with Pure Pursuit and MPC using different total timesteps. Modified trajectories and horizon trajectories are marked in red and yellow. Lookahead points are shown in cyan in Pure Pursuit plots.

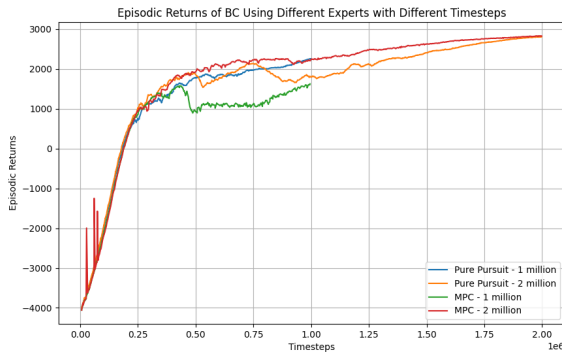


Fig. 6: Episodic returns of BC for path-tracking with Pure Pursuit and MPC demonstrations with different training timesteps.

This model is configured with a 2 s prediction time and trained over a total of 2 million timesteps. To create an obstacle map, we modify the original obstacle-free map by adding 2, 3, and 4 static obstacles respectively. Each obstacle box measures 7×7 pixels, approximately 35×35 cm, which side length is a full width of an FITENTH car in real scenarios. The obstacles are strategically placed along the waypoints to evaluate the vehicle’s nudging performance.

For the nudging performance, we use 10 million total timesteps to train the aforementioned model. The actual performances are shown in Fig. 7. Lateral offsets \mathbf{o} successfully modify the horizon trajectory \mathbf{t}_h truncated from reference waypoints to get a new modified trajectory \mathbf{t}_m , which is then taken by Pure Pursuit, the path-tracking controller for actual maneuver. Here, Pure Pursuit calculates a lookahead point to guide the vehicle avoiding the obstacles using \mathbf{t}_m . The corresponding episodic returns shown in Fig. 7 increase throughout the training process, depicting the convergence of the policies through trial and errors.

IV. CONCLUSION

In this work, we introduce the method that uses BC and PPO algorithms for trajectory planning tasks, specifically path-tracking and static obstacle nudging. Our experiments in the FITENTH Gym environment validate that this method

effectively performs both path-tracking using BC and fixed obstacle nudging using PPO bootstrapped by BC. The development demonstrates the efficacy of integrating learning into planning and highlights the practical benefits of combining RL with IL in the field of autonomous driving. Future work will focus on reducing the sim-to-real gap for robust deployment, stronger generalizability to various kinds of dynamic obstacles, and decoupling the planning from decision-making to physics-constrained motion planning.

V. ACKNOWLEDGEMENT

The authors express their sincere gratitude to Tian Tan from the Department of the Electrical and Systems Engineering, the University of Pennsylvania, for his dedicated assistance with the experiments. We also extend our thanks to Yi Shen from the Robotics Department at the University of Michigan for his helpful discussions and advice.

REFERENCES

- [1] R. S. Sutton, D. McAllester, S. Singh, and Y. Mansour, “Policy gradient methods for reinforcement learning with function approximation,” *Advances in neural information processing systems*, vol. 12, 1999.
- [2] J. Schulman, S. Levine, P. Abbeel, M. Jordan, and P. Moritz, “Trust region policy optimization,” in *International conference on machine learning*. PMLR, 2015, pp. 1889–1897.
- [3] J. Schulman, F. Wolski, P. Dhariwal, A. Radford, and O. Klimov, “Proximal policy optimization algorithms,” *arXiv preprint arXiv:1707.06347*, 2017.
- [4] A. Hussein, M. M. Gaber, E. Elyan, and C. Jayne, “Imitation learning: A survey of learning methods,” *ACM Computing Surveys (CSUR)*, vol. 50, no. 2, pp. 1–35, 2017.
- [5] C. Sammut, *Behavioral Cloning*. Boston, MA: Springer US, 2010, pp. 93–97. [Online]. Available: https://doi.org/10.1007/978-0-387-30164-8_69
- [6] S. Ross, G. Gordon, and D. Bagnell, “A reduction of imitation learning and structured prediction to no-regret online learning,” in *Proceedings of the fourteenth international conference on artificial intelligence and statistics*. JMLR Workshop and Conference Proceedings, 2011, pp. 627–635.
- [7] M. Kelly, C. Sidrane, K. Driggs-Campbell, and M. J. Kochenderfer, “Hg-dagger: Interactive imitation learning with human experts,” in *2019 International Conference on Robotics and Automation (ICRA)*. IEEE, 2019, pp. 8077–8083.
- [8] J. Spencer, S. Choudhury, M. Barnes, M. Schmittle, M. Chiang, P. Ramadge, and S. Srinivasa, “Expert intervention learning,” *Autonomous Robots*, vol. 46, no. 1, pp. 99–113, 2022.
- [9] X. Sun, Y. Wu, S. Bhattacharya, and V. Kumar, “Multi-agent exploration of an unknown sparse landmark complex via deep reinforcement learning,” 2022. [Online]. Available: <https://arxiv.org/abs/2209.11794>

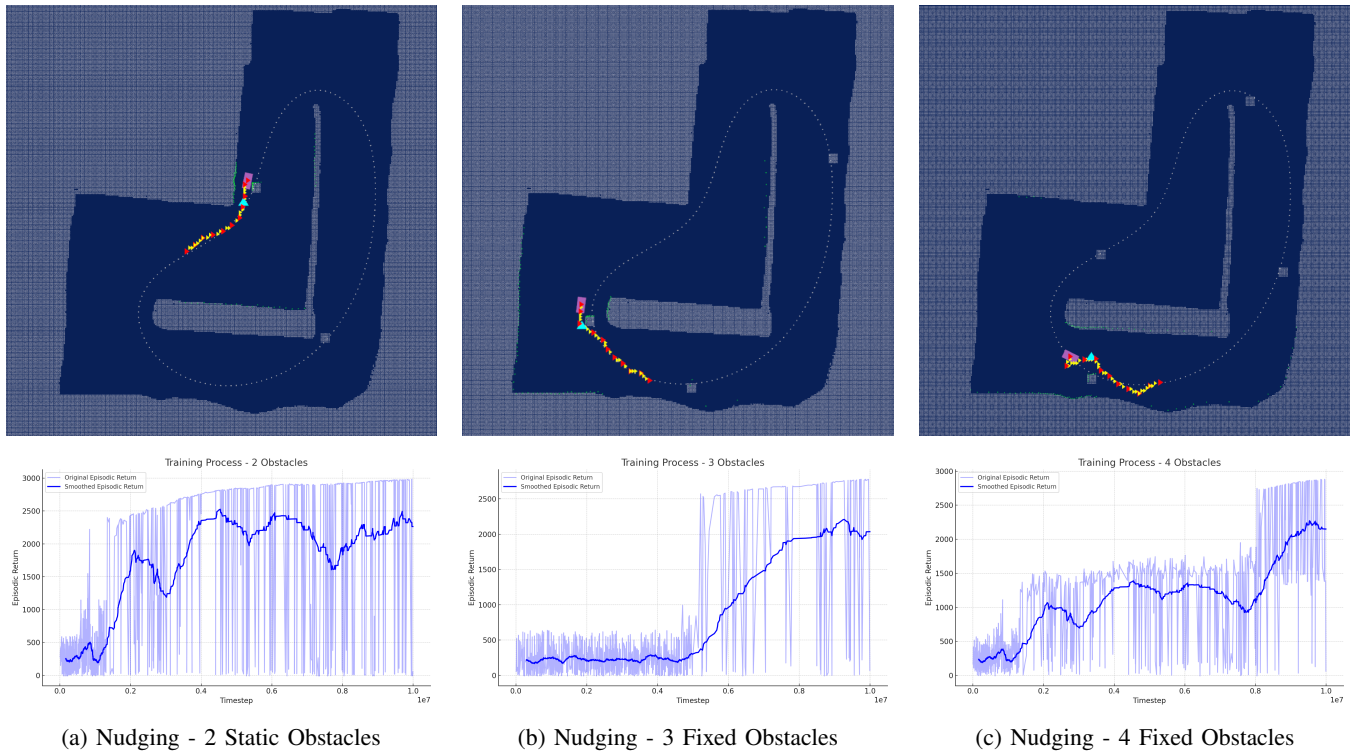


Fig. 7: Static obstacle nudging and corresponding episodic returns using BC-bootstrapped PPO with Pure Pursuit validated with different fixed obstacle setups. Modified trajectories are marked in red triangles and yellow lines. Cyan triangles denote the lookahead points.

- [10] H. Liu, Y. Shen, W. Zhou, Y. Zou, C. Zhou, and S. He, “Adaptive speed planning for unmanned vehicle based on deep reinforcement learning,” 2024. [Online]. Available: <https://arxiv.org/abs/2404.17379>
- [11] Y. Zhang, K. Mo, F. Shen, X. Xu, X. Zhang, J. Yu, and C. Yu, “Self-adaptive robust motion planning for high dof robot manipulator using deep mpc,” *arXiv preprint arXiv:2407.12887*, 2024.
- [12] Y. Pan, C.-A. Cheng, K. Saigol, K. Lee, X. Yan, E. Theodorou, and B. Boots, “Agile autonomous driving using end-to-end deep imitation learning,” in *Robotics: Science and Systems XIV*. Robotics: Science and Systems Foundation, June 2018. [Online]. Available: <https://doi.org/10.15607/rss.2018.xiv.056>
- [13] P. Cai, H. Wang, H. Huang, Y. Liu, and M. Liu, “Vision-based autonomous car racing using deep imitative reinforcement learning,” *IEEE Robotics and Automation Letters*, pp. 1–1, 2021.
- [14] M. OKelly, H. Zheng, D. Karthik, and R. Mangharam, “F1tenth: An open-source evaluation environment for continuous control and reinforcement learning,” in *Proceedings of the NeurIPS 2019 Competition and Demonstration Track*, ser. Proceedings of Machine Learning Research, vol. 123. PMLR, 2020, pp. 77–89. [Online]. Available: <http://proceedings.mlr.press/v123/o-kelly20a.html>
- [15] J. Becker, N. Imholz, L. Schwarzenbach, E. Ghignone, N. Baumann, and M. Magno, “Model- and acceleration-based pursuit controller for high-performance autonomous racing,” in *2023 IEEE International Conference on Robotics and Automation (ICRA)*, 2023, pp. 5276–5283.
- [16] M. Bosello, R. Tse, and G. Pau, “Train in austria, race in montecarlo: Generalized rl for cross-track f1 tenth lidar-based races,” in *2022 IEEE 19th Annual Consumer Communications & Networking Conference (CCNC)*. IEEE, 2022, pp. 290–298.
- [17] X. Sun, S. Yang, M. Zhou, K. Liu, and R. Mangharam, “Mega-dagger: Imitation learning with multiple imperfect experts,” 2024. [Online]. Available: <https://arxiv.org/abs/2303.00638>
- [18] J. Betz, H. Zheng, A. Liniger, U. Rosolia, P. Karle, M. Behl, V. Krovi, and R. Mangharam, “Autonomous vehicles on the edge: A survey on autonomous vehicle racing,” *IEEE Open Journal of Intelligent Transportation Systems*, 2022.
- [19] Z. Qiao, M. Zhou, Z. Zhuang, T. Agarwal, F. Jahncke, P.-J. Wang, J. Friedman, H. Lai, D. Sahu, T. Nagy, M. Eandler, J. Schlessman, and R. Mangharam, “Av4ev: Open-source modular autonomous electric vehicle platform for making mobility research accessible,” 2024. [Online]. Available: <https://arxiv.org/abs/2312.00951>
- [20] Z. Zhuang, “f1tenth_rl,” https://github.com/zzjun725/f1tenth_rl, 2024.
- [21] X. Sun, M. Zhou, Z. Zhuang, S. Yang, J. Betz, and R. Mangharam, “A benchmark comparison of imitation learning-based control policies for autonomous racing,” in *2023 IEEE Intelligent Vehicles Symposium (IV)*, 2023, pp. 1–5.
- [22] V. Sezer and M. Gokasan, “A novel obstacle avoidance algorithm: “follow the gap method”,” *Robotics and Autonomous Systems*, vol. 60, no. 9, pp. 1123–1134, 2012. [Online]. Available: <https://www.sciencedirect.com/science/article/pii/S0921889012000838>
- [23] T. Weiss and M. Behl, “Deepracing: Parameterized trajectories for autonomous racing,” *arXiv preprint arXiv:2005.05178*, 2020.
- [24] L. Lipeng, L. Xu, J. Liu, H. Zhao, T. Jiang, and T. Zheng, “Prioritized experience replay-based ddqn for unmanned vehicle path planning,” *arXiv preprint arXiv:2406.17286*, 2024.
- [25] J. M. Snider *et al.*, “Automatic steering methods for autonomous automobile path tracking,” *Robotics Institute, Pittsburgh, PA, Tech. Rep. CMU-RI-TR-09-08*, 2009.
- [26] A. Heilmeyer, A. Wischniewski, L. Hermansdorfer, J. Betz, M. Lienkamp, and B. Lohmann, “Minimum curvature trajectory planning and control for an autonomous race car,” *Vehicle System Dynamics*, vol. 58, no. 10, pp. 1497–1527, 2020. [Online]. Available: <https://doi.org/10.1080/00423114.2019.1631455>
- [27] S. Huang, R. F. J. Dossa, C. Ye, J. Braga, D. Chakraborty, K. Mehta, and J. G. Araújo, “Cleanrl: High-quality single-file implementations of deep reinforcement learning algorithms,” *Journal of Machine Learning Research*, vol. 23, no. 274, pp. 1–18, 2022. [Online]. Available: <http://jmlr.org/papers/v23/21-1342.html>
- [28] R. Rajamani, *Vehicle Dynamics and Control*. New York: Springer, 2012.